A Geospatial Approach to Wildfire Risk Modeling Using Machine Learning and Remote Sensing Data

Riya Gupta and Hudson Kim

***Abstract*—In recent years, the likelihood of wildfire occurrence has increased in many North American communities as changes in climate have led to longer, more deadly fire seasons. Many Americans, especially those living in Western states, have reported frequent drought and wildfire conditions, leading to an increased need for a modeling program to assess wildfire risk at a low computational cost. The research objective of this article was to develop a machine-learning model capable of producing the accurate wildfire risk assessments using five geospatial datasets: Land fire mean return, annual precipitation, Sentinel-2 imagery, land cover, and moisture deficit and surplus. To create the model, three separate machine-learning architectures were implemented (U-Net, DeepLabV3, and the pyramid scene parsing network) and then applied to the study area of San Bernardino County, CA, for the year of 2020. This study demonstrated a proof of concept for further inquiry into combining artificial intelligence and geospatial datasets to create useful insights.**

***Index Terms*—Deep learning, geophysical data, natural disasters and hazard, optical data.**

I. Introduction

SINCE California's first recorded wildfire in 1889, there has been a significant increase in the frequency of wildfires throughout the state. The increasing risk of wildfires has contributed to higher levels of inhalable particulate matter, placing an economic and health strain on local communities [1]. As wildfires continue to threaten California residents, the accurate wildfire prediction models are crucial for managing fire response assets and addressing wildfire trends. Moreover, these wildfire modeling systems must be cost-efficient in order to be accessible to the general public regardless of economic status [2]. Yet, there is limited application of machine-learning models for wildfire risk prediction and few have been developed to produce an output that is economically feasible, accurate, and easily available to communities with frequent fire occurrence [3].

II. Literature Review

In recent years, the development of high-resolution satellite imagery from sources, such as the Aqua and Terra satellites, has opened the possibility of developing an efficient and accurate wildfire risk modeling framework [4], [5]. Such frameworks support wildfire preparedness, one of the four components of wildfire management, through greater satellite data accessibility to support the development of a predictive model [6]. When taking data from a satellite source and applying it to a geospatial machine-learning model, the accuracy of the results depends on the quality of the datasets used to train the model. Scott et al. [7] presented an open-source wildfire hazard potential (WHP) map, which provides further research into wildfire risk forecasting based on population density, building coverage, housing unit density, building exposure type, housing unit exposure, housing unit impact, and housing unit risk updated yearly. With its results, this dataset provided promise in being used as a ground truth data layer to help train a model with similar input factors.

Several studies have been conducted using various physics-based parameters and environmental factors to model the growth and spread of fire during a wildfire event. In June 2022, a study conducted in London used inverse modeling based on latent assimilation techniques to estimate the parameters of a wildfire, finding that machine-learning-driven prediction models created a precise reconstruction of test datasets [8]. Additionally, a number of studies have applied deep learning to create datasets that combine environmental factors, such as topography, weather, and vegetation [9]. These maps can be implemented into algorithms that predict various wildfire risk aspects, such as fire spread and ignition.

The reliability of such models relies on the accuracy and precision of data points used in the datasets fueling the algorithm. While wildfire spread and evolution have been critically monitored for decades, limited access to large datasets hinders the prediction of wildfire behavior [10]. The inherent lack of substantial geospatial imagery layers poses a challenge when creating a predictive wildfire model as a substantial number of inputs are required to develop intelligent algorithms that can handle unseen data [11]. This issue is compounded by the variations in classes that each dataset has, as geospatial imagery layers inherently cover diverse geographies, creating variations in the number of classes each dataset has during model training. Class imbalances decrease the performance quality of a model, fueling misguided research with inaccurate results [12].

Within wildfire prediction, class imbalances exist within a geographic region as areas do not have equal coverage of fire risk. To create a model that can be adapted to wide geographic areas, a model must be trained on large datasets that are balanced for each risk class to prevent biases where a model prefers one class

Manuscript received 8 December 2023; revised 15 April 2024 and 13 July 2024; accepted 13 July 2024. Date of publication 26 July 2024; date of current version 8 August 2024. This work was supported by NASA STEM Enhancement in the Earth Science (SEES) Program. *(Hudson Kim and Riya Gupta are co-first authors.) (Corresponding author: Riya Gupta.)*

Riya Gupta is with the Northwood High School, Irvine, CA 92620 USA (e-mail: riya@budakia.com).

Hudson Kim is with the Westview High School, San Diego, CA 92129 USA (e-mail: hudson.n.kim@gmail.com).

Digital Object Identifier 10.1109/JSTARS.2024.3434368

result over another. Given the lack of available data for wildfire prediction modeling, it becomes necessary to implement data augmentation techniques to enhance the variety and quantity of data available to train a model and resolve class imbalances [13].

With the wide variety of data augmentation techniques available, certain methods are better suited to solving certain machine-learning problems. Currently, wildfire modeling often relies on either random oversampling or random undersampling as the primary data augmentation technique [14], [15]. Oversampling and undersampling are both implemented when one class within a dataset has a much larger number of samples compared with other classes. For oversampling, the dataset is balanced by magnifying the minority classes by creating artificial examples or duplicating existing data points. Similarly, for undersampling, the over-represented class has data points removed until it has an equal number of examples compared with all classes. However, by removing or creating replications of existing data, training samples lose significant patterns that can allow models to accurately handle unseen data, increasing the risk of model overfitting [16], [17].

Based on the disadvantages of oversampling and undersampling, an over-reliance on such processes creates a gap in the field of wildfire predictive modeling to apply better suited data augmentations that do not rely on oversampling or undersampling to rebalance classes. For such modeling, ongoing research suggests that transforms, such as dihedral affines, are better suited as they can expand a dataset without losing key visual features [18]. As such, a crucial target of this research was to apply such data augmentation techniques to improve the accuracy of current state-of-the-art wildfire prediction modeling.

In addition to proper data augmentation, the accurate results also require datasets that reflect a study area's changing climate conditions and local ecology. With the rapid acceleration of climate change in recent years, past wildfire prediction models have become inadequate in predicting risk due to the reliance on datasets that no longer mirror modern trends in weather patterns, wind intensity, soil composition, etc. [19]. When creating a tool to predict wildfires with current climate conditions considered, factors, such as fire regimes, need to be taken into consideration in order to more accurately depict the environment in which a wildfire prediction model is being trained for and run.

The objective of this study is to compare three machine-learning models to propose an effective machine-learning methodology for wildfire risk prediction that is uniquely adaptable to a changing ecology and environment through the novel application of relatively new data augmentations. This model is aimed to be applicable over a large geographical area in future applications, such as over the entire United States.

III. Study Area

A. Study Area

San Bernardino County was selected because the county's land area includes a variety of high and low wildfire risk extremes according to the United States Department of Agriculture (USDA) hazard potential map. This will allow us to test the model in several scenarios. Along with this, San Bernardino County encompasses the San Bernardino National Forest, allowing for forest fire risk assessment, inspired by Cheng et al. [20].

IV. Methodology

A. Data Selection

The training process involved five different input sets: Land fire mean return, historic annual precipitation, Sentinel-2 imagery, land cover, and moisture deficit and surplus imagery (see Fig. 1), all of which were stacked together into a single composite layer to enable faster training times. Additionally, before training, several augmentation steps were run to expand the training dataset and expose the model to more varied conditions, including rotations, brightness changes, contrast modifications, zooms, and crops. Uniquely the dihedral affine augmentation that rotates an image in the eight possible directions of a dihedron while retaining points and straight lines was also implemented. This data augmentation is especially well-suited for wildfire prediction due to its varied adjustments to geospatial data that reflect common environmental factors, such as haze or clouds, while still retaining important visual features. An image of the stacked data layers is provided in image 6 of Fig. 1. This image shows the stacked layers prior to the augmentation steps taken to expand the dataset.

The first base layer is the land fire mean return layer. Provided by the USDA, the land fire mean return input layer quantifies the average number of years between fire occurrences in a geographic area [21]. This is useful for risk assessment as fire intervals provide insight into the ecological conditions and fire regimes of a specific area [22].

The second dataset used was the historical annual precipitation dataset. Developed by the USDAs Rocky Mountain Research Station, this dataset includes precipitation, air temperature, snow, and stream flow data throughout San Bernardino County. The data were used to discern unburnable land areas (rivers, streams, lakes, etc.) throughout San Bernardino County and understand the moisture content throughout the area, which is correlated to wildfire potential [23].

The European Space Agency's Sentinel-2 imagery layer was also used to provide a visual perspective of the study area [24]. This was done in order to provide the model with a better understanding of the geographic and topographical environment of San Bernardino County with data that is frequently updated with new information.

The moisture deficit and surplus layer uses moisture difference z-score datasets to analyze the distance of moisture content values from the calculated mean [25]. This dataset was implemented to gain insight into the implications of moisture conditions, such as drought, which can impact wildfire risk.

Finally, the land cover layer, which includes various classifications of land objects, such as water bodies, tree clusters, flooded vegetation, crops, human-developed areas, bare ground, snow/ice, and cloud-covered areas, was included to provide more context to the underlying geography [26].

Once the input layers were established, the USDA WHP map was selected to be the ground truth output layer [7]. This dataset is an index that identifies geographical areas in which a

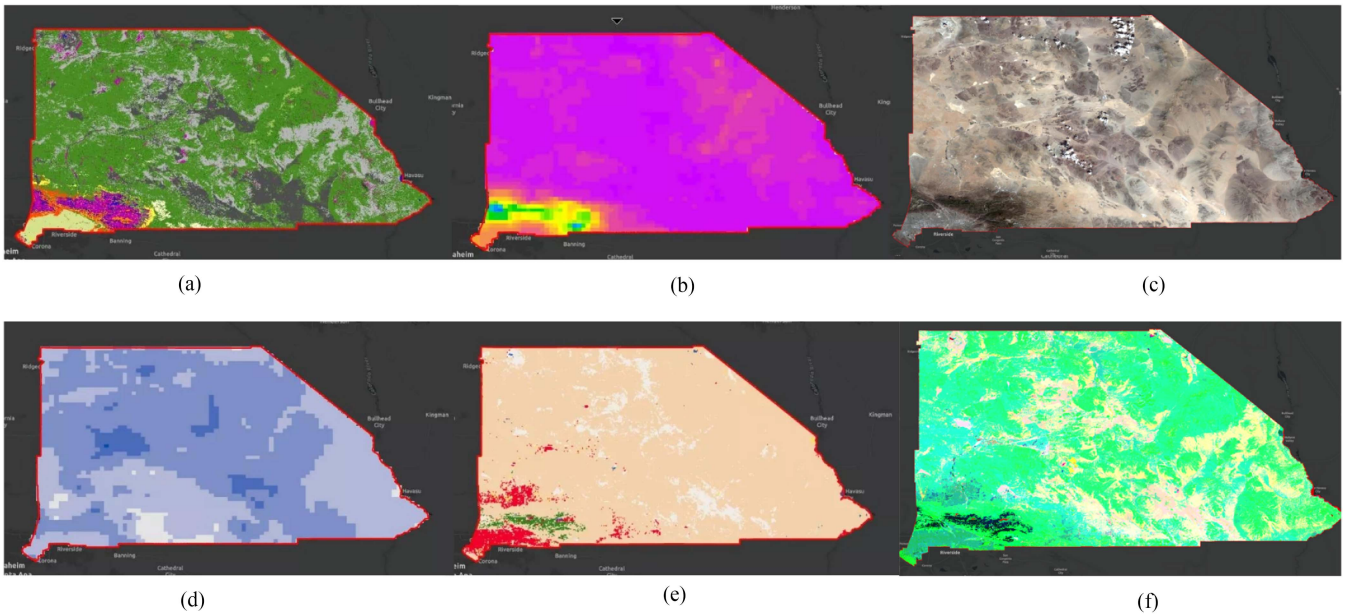

Fig. 1. Input layers and combined composite layer used to train the machine-learning model. (a) Land fire mean return imagery layer. (b) Precipitation imagery layer. (c) Sentinel-2 imagery layer. (d) Moisture deficit and surplus imagery layer. (e) Land cover imagery layer. (f) Composite layer of all input layer.

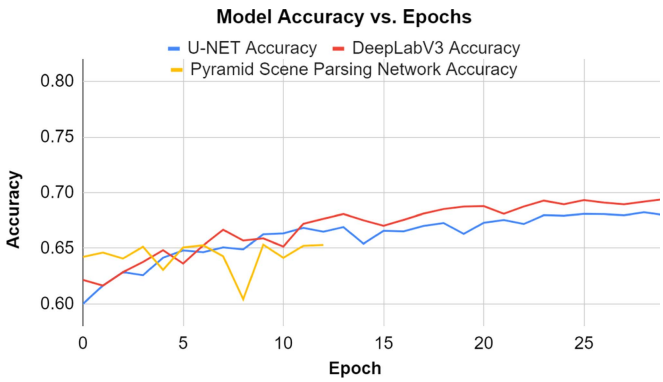

Fig. 2. Graph of U-Net, DeepLabV3, and PSPNet's accuracy over the number of epochs.

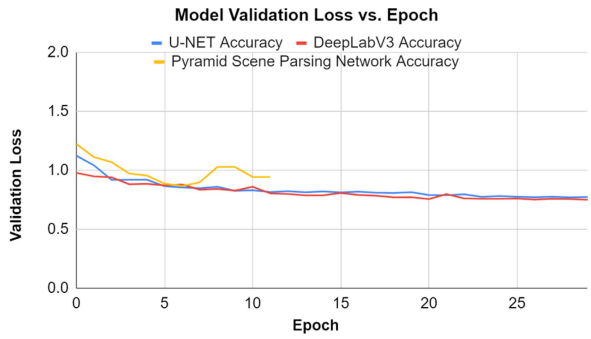

Fig. 3. Graph of U-Net, DeepLabV3, and PSPNet's validation loss over the number of epochs.

wildfire will be difficult to contain with standard fire suppression techniques. The wildfire modeling data used for the WHP are based upon data collected from the USDAs 2020 assessment of wildfire risk factors and components.

B. Annotation Process and Class Names

To classify wildfire risk, the USDAs forest service WHP map's seven distinct class names were used: Very low risk, low risk, moderate risk, high risk, very high risk, nonburnable, and water. Using these labels, a total of 56 440 samples were created for model training.

C. Model Architecture

For the model architecture, three separate models were selected for their efficiency and relatively high accuracy. They are U-Net, DeepLabV3, and pyramid scene parsing network (PSPNet).

1) U-Net: Unlike traditional convolutional neural networks (CNNs), the U-Net is a symmetric model composed of two major segments [27]. The leftmost segment is known as the contracting path, and the rightmost part is known as the expansive path. In the contracting path, the high-level features are captured using a series of convolution and pooling layers. Convolutional layers are responsible for extracting features, while pooling layers lower the spatial dimensions of the features. On the other side, the decoding path takes the encoded features and upsamples them to the original image size. This is done through a series of upsampling layers and convolutional layers. Importantly, the U-Net utilizes several skip connections that bridge the encoding and decoding paths at several levels. By doing so, the network is able to retain crucial information, such as the location of specific features from the previous layers. Based on these features, the U-Net is a powerful pixel classification model well-suited for classifying and determining wildfire risk.

2) DeepLabV3: The second model architecture tested was the DeepLabV3 model architecture. At its core, DeepLabV3 has three main parts: a base-level encoder (this study used Resnet-34), an atrous spatial pyramid pooling (ASPP)

TABLE I
U-NET, DEEPLABV3, AND PSPNET'S *F*1-SCORES

Model	F1 score
U-Net	0.993781
DeepLabV3	0.991178
Pyramid Scene Parsing Network (PSPNet)	0.985348

TABLE II
U-NET, DEEPLABV3, AND PSPNET'S PRECISION AND RECALL SCORES FOR "VERY LOW" WILDFIRE RISK CATEGORY

Model	Precision	Recall
U-Net	0.99063	0.996952
DeepLabV3	0.986675	0.995722
Pyramid Scene Parsing Network	0.97848	0.992314

module, and a decoder. The encoder portion of the model extracts high-level features and general contextualization from the input image through a multitude of convolution and pooling layers. From there, the ASPP module is applied to capture multiscaled information. Using parallel atrous convulsions with varying dilation rates, the ASPP module is able to capture fine-grained details and the broader context of the image. Finally, a decoder is applied that refines the output of the ASPP module and generates a pixelwise segmentation map. This is achieved through bilinear upsampling and skip connections that recover spatial resolution lost in the encoding process. Compared with other existing models, DeepLabV3 has a mean intersection of union score of 86.90%, signifying a low pixel-by-pixel error rate between a model's predicted output and the ground truth data. Other models, such as the TuSimple and ResNet-38, score slightly less with 83.10% and 80.60%, respectively, making DeepLabV3 a good choice for wildfire risk prediction for the model [28].

3) Pyramid Scene Parsing Network: The final model architecture implemented was the PSPNet. Similar to the DeepLabV3 and U-Net models, the PSPNet is composed of an encoder and decoder. The encoder utilizes a CNN backbone model and several dilated convolutions in later layers to understand the global context within the input layers. Uniquely, the PSPNet incorporates a pyramid pooling module, which pools various features at multiple scales, applies convolutions, and upsamples the features to aggregate contextual information and improve segmentation accuracy [29]. Once the encoder has finished, the decoder takes the features extracted and predicts the class(es) of every pixel. Within the PSPNet, two main options exist for the decoder: an 8× upsampling decoder with bilinear upsampling, or a U-Net-like decoder, which uses skip connections to bring lower level features from the encoder to the decoder. On the rendering side, the PSPNet utilizes a technique known as PointRend, which enables crisp segmentation boundaries [30]. This is accomplished by using a point-based rendering neural network module to predict labels for selected points, as compared with upsampling on a regular grid.

TABLE III
INDIVIDUAL CLASSIFICATION MODEL METRICS FOR U-NET MODEL

	Very Low	Low	Moderate	High	Very High
Precision	0.9906	0.6650	0.3359	0.6492	0.7921
Recall	0.9969	0.6918	0.4375	0.5413	0.8454
***F*1 Score**	0.9937	0.6782	0.3800	0.5904	0.8179

D. Model Training

Each model was run for 30 epochs using ArcGIS Pro's train deep learning model tool. A total of 30 epochs were experimentally determined to be optimal, as for the past 30 epochs, the model's performance did not improve. For each epoch, model statistics were computed, in particular, training_loss, validation_loss, accuracy, and dice.

V. RESULTS

Across all models, several metrics were recorded, including model accuracy, as shown in Fig. 2. Notably, the PSPNet in all model metrics stopped training around 12 epochs as it stopped improving and plateaued.

Additionally, each model's *F*1-score was calculated detailed in Table I. Within the realm of machine learning, an *F*1-score measures a model's accuracy as a harmonic mean of precision and recall. A precision score indicates the false positive predictions for a model, while a recall score indicates the frequency with which the model correctly identifies true positives from the layers

$$F1 = \frac{\text{True Positive}}{\text{True Positive} + \frac{1}{2}(\text{False Positive} + \text{False Negative})}. \tag{1}$$

Along with each model's *F*1-score, precision and recall scores were calculated using the equations as follows. The precision and recall scores are a useful tool for providing a basis for comparison with other existing models

$$\text{Precision} = \frac{\text{True Positives}}{\text{True Positives} + \text{False Positives}} \tag{2}$$

$$\text{Recall} = \frac{\text{True Positives}}{\text{True Positives} + \text{False Negatives}}. \tag{3}$$

Table II reflects the precision and recall scores for each respective model architecture for the "Very Low" wildfire risk category. From this table, the U-Net model architecture had the greatest precision score with a score of 0.99063, while the PSPNet had the lowest score of 0.97848.

Table III outlines precision, recall, and *F*1 results for each of the five class levels implemented within the U-Net architecture, which was the best out of the three models trained. Based on these results, the U-Net model had the highest results in

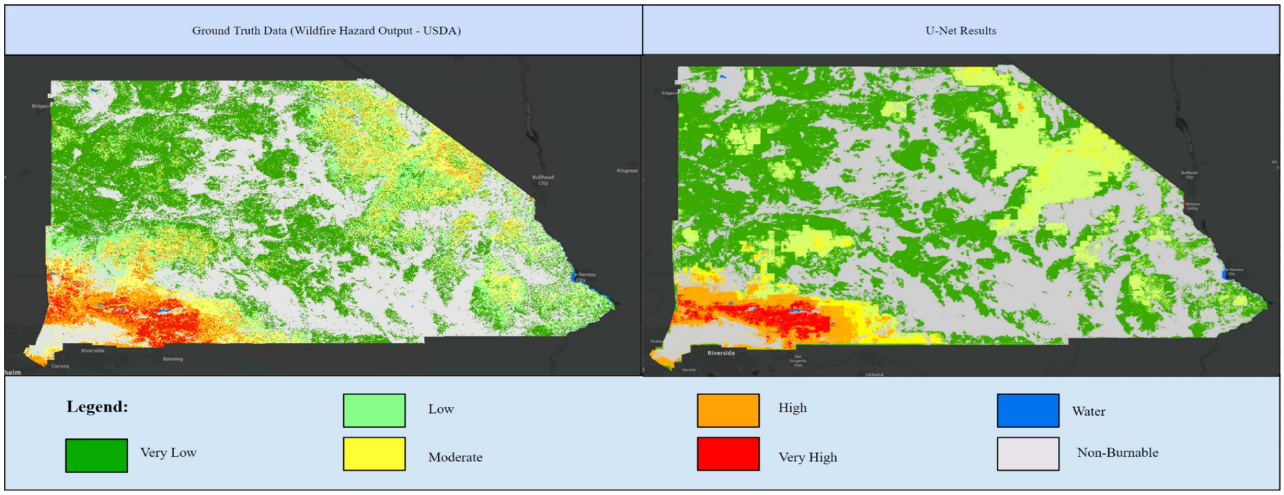

Fig. 4. Example classification results from U-Net versus the ground truth data from the USDA wildfire hazard output.

the "Very Low" wildfire classification category with precision, recall, and $F1$-scores of 0.9906, 0.9969, and 0.9937, respectively. Conversely, the U-Net model had the lowest results in the "Moderate" category with precision, recall, and $F1$-scores of 0.3359, 0.4375, and 0.3800, respectively.

Finally, throughout the entire training process, each model's validation loss was also calculated, as shown in Fig. 3 and compared to the ground truth data in Fig. 4.

VI. Discussion

When compared with previous studies, the U-Net model outperformed the ResNet-50 model from the Wang et al.'s [31] study, which predicted wildfire progressions and road extractions. This suggests a progression in wildfire predictive technology, allowing it to be applicable in a practical setting. Additionally, the U-Net model had a greater precision and recall performance when compared with the Farasin et al.'s [32] study, which used a U-Net architecture to identify burned and unburned areas in Portugal, Spain, France, Italy, and Sweden. However, this work on wildfire prediction analyzed an area once it had been burned, setting the model in this article apart in applying a similarly large array of datasets for a truly predictive model.

Furthermore, the model developed through this research was compared with various existing products to understand the implications of applying novel data augmentations, such as dihedral affine, which have not been standardized throughout wildfire predictive modeling. In particular, the dihedral affine data augmentation is useful for wildfire modeling as it exposes a model to more varied edge cases while still retaining important visual features. This is in contrast to other data augmentations present in previous studies where augmentations, such as pure rotations lose or distort important visual markers needed for wildfire prediction.

In comparison with a similar research, the predictive model from this article was found to have higher performance metrics. For example, Pérez-Porras et al. [33] utilized oversampling and undersampling to create six predictive classifiers that identified wildfire risk in southern Spain. When comparing the results of Pérez-Porras et al. to the models developed in this research, the $F1$-scores of Pérez-Porras et al. are substantially lower between 0.42 and 0.57 than that of the U-Net, DeepLabV3, and PSPNet individually, all of which had higher than 0.9 $F1$-scores in the "Very Low" class.

Similarly, another example of an existing comparable product is Kondylatos et al.'s study [34], which implemented several different model architectures to predict wildfire risk. Their highest performing model for precision was the ConvLSTM, which had a 0.923 precision score. Their highest performing recall model was LSTM, which had a score of 0.755. Finally, their greatest $F1$-score model was ConvLSTM, which had a score of 0.806. When compared with the results from this article, the results of Kondylatos et al.'s study had lower metric scores despite having fewer training samples, 40 554 samples versus 56 440 samples in this study.

Additionally, Seddouki et al. [35] applied a similar methodology by considering ecological factors when applying datasets for a machine-learning model that predicts forest fire susceptibility. Following their study, Seddouki et al. established the precision of their random forest model to be 0.891, which is significantly lower than the precision scores for all three models developed throughout this article. A crucial difference in Seddouki et al.'s article when compared with the methodology of this article is the data processing and augmentation process because Seddouki et al. used a smaller training sample size (428) while also not applying significant data augmentations to offset natural biases within their dataset.

Despite these promising statistics, it is important to acknowledge the limitations of this study. While the datasets had many individual data points within the target study area, there are still gaps within data as a result of incomplete input datasets. Such missing data can generate minor inaccuracies within the precision of each model [36]. While it is difficult to select a dataset that contains no missing values, the quality of a dataset can be improved through enhanced satellite imagery collection.

Moreover, when discussing the area analyzed, the study area was limited to San Bernardino County, which may lack the

ecosystem diversity to account for edge cases in other parts of the United States. For training purposes, it was challenging to incorporate a larger area while accounting for the limited computing power of an NVIDIA 1060 GPU. In the future, an expansion of the research area to include the rest of California or the entire United States may be sought after.

VII. Conclusion

This is one of the first studies of its kind to create a wildfire prediction model using dihedral affine among other data augmentations on five separate large geospatial datasets in San Bernardino County, CA [37]. Notably, the incorporation of the USDA's land fire mean return input layer enables the model to include environmental fire regimes into risk calculations, allowing for a multidimensional analysis that takes into consideration the changing ecology of a landscape throughout time. This allows for more applicable forecasting that is relevant to prediction needs in the age of climate change.

When applied, this modeling technology can support conservation efforts by decreasing uncertainties in aerosol emissions, vegetation succession, nutrient cycling, and species diversity in various ecosystems [38], [39], [40], [41].

Overall, this study offers robust geospatial insights, underlining the potential for developing cost-effective wildfire risk prediction models. By harnessing the data generated by this model, policymakers and local fire departments cannot only foster heightened public awareness about wildfire preparedness but also strategically allocate wildfire resources to where they are most urgently needed.

Acknowledgment

NASA STEM Enhancement in the Earth Science (SEES) Program is led by the Texas Space Grant Consortium (TSGC) at the University of Texas at Austin (NASA Award NNX16AB89A), and TSGC is funded through the NASA National Space Grant College and Fellowship Program (Space Grant) Training Grant. The Urban Heat Island and Air Quality Internship is a part of GLOBE Mission Earth (NASA Award NNX16AC54A S007). This work was mentored by Dr. K. Czajkowski and Dr. Y. Jiang of the University of Toledo.

References

[1] G. Chen et al., "Mortality risk attributable to wildfire-related PM2·5 pollution: A global time series study in 749 locations," *Lancet Planet. Health*, vol. 5, pp. e579–e587, Sep. 2021, doi: 10.1016/S2542-5196(21)00200-X.

[2] M. Hino and C. B. Field, "Fire frequency and vulnerability in California," *PLoS Climate*, Feb. 2023, Art. no. e0000087, doi: 10.1371/journal.pclm.0000087.

[3] J. Burrell, "How the machine 'thinks': Understanding opacity in machine learning algorithms," *Big Data Soc.*, vol. 3, pp. 1–12, Jan. 2016, doi: 10.1177/205395171562251.

[4] P. Jain, S. C. P. Coogan, S. G. Subramanian, M. Crowley, S. Taylor, and M. D. Flannigan, "A review of machine learning applications in wildfire science and management," *Environ. Rev.*, vol. 28, no. 4, pp. 478–505, Dec. 2020, doi: 10.1139/er-2020-0019.

[5] C.-L. C. Huang and T. Munasinghe, "Exploring various applicable techniques to detect smoke on the satellite images," in *Proc. IEEE Int. Conf. Big Data*, 2020, pp. 5703–5705, doi: 10.1109/BigData50022.2020.9378466.

[6] C. Tymstra, B. J. Stocks, X. Cai, and M. D. Flannigan, "Wildfire management in Canada: Review, challenges and opportunities," *Prog. Disaster Sci.*, vol. 5, Jan. 2020, Art. no. 100045, doi: 10.1016/j.pdisas.2019.100045.

[7] J. H. Scott, A. M. Brough, J. W. Gilbertson-Day, G. K. Dillon, and C. Moran, "Wildfire risk to communities: Spatial datasets of wildfire risk for populated areas in the United States," U.S. Department of Agriculture, 2020. [Online]. Available: https://www.fs.usda.gov/rds/archive/catalog/RDS-2020-0060

[8] S. Cheng et al., "Parameter flexible wildfire prediction using machine learning techniques: Forward and inverse modelling," *Remote Sens.*, vol. 14, no. 13, Jul. 2022, Art. no. 3228, doi: 10.3390/rs14133228.

[9] D. Shadrin et al., "Wildfire spreading prediction using multimodal data and deep neural network approach," *Sci. Rep.*, vol. 14, 2024, Art. no. 2606, doi: 10.1038/s41598-024-52821-x.

[10] Q. E. Barber et al., "The Canadian fire spread dataset," *Nature*, vol. 11, Jul. 2024, Art. no. 764, doi: 10.1038/s41597-024-03436-4.

[11] E. Alpaydin, "Why are we interested in machine learning?," in *Machine Learning*. Cambridge, MA, USA: MIT Press, 2016.

[12] Q. Gu, Z. Cai, L. Zhu, and B. Huang, "Data mining on imbalanced data sets," in *Proc. Int. Conf. Adv. Comput. Theory Eng.*, 2008, pp. 1020–1024, doi: 10.1109/ICACTE.2008.26.

[13] A. Mumuni and F. Mumuni, "Data augmentation: A comprehensive survey of modern approaches," *Array*, vol. 16, Dec. 2022, Art. no. 100258, doi: 10.1016/j.array.2022.100258.

[14] J. Florath and S. Keller, "Supervised machine learning approaches on multispectral remote sensing data for a combined detection of fire and burned area," *Remote Sens.*, vol. 14, no. 3, Jan. 2022, Art. no. 657, doi: 10.3390/rs14030657.

[15] P. Kaur, "Forest fire prediction using heterogeneous data sources and machine learning methods," M.S. thesis, Dept. Comput. Sci., Univ. of Waterloo, Waterloo, ON, Canada, 2023.

[16] Á. Griño, "Machine learning algorithms to predict wildfire propagation in Europe," M.S. thesis, Dept. Telecomm. Tech., Barcelona Tech., Barcelona, Spain, 2021.

[17] A. S. Tarawneh, A. B. Hassanat, G. A. Altarawneh, and A. Almuhaimeed, "Stop oversampling for class imbalance learning: A review," *IEEE Access*, vol. 10, pp. 47643–47660, 2022, doi: 10.1109/ACCESS.2022.3169512.

[18] FastAI, "Vision.transform list of transforms for data augmentation in CV," Source, 2023. [Online]. Available: https://fastai1.fast.ai/vision.transform.html

[19] H. An, J. Gan, and S. J. Cho, "Assessing climate change impacts on wildfire risk in the United States," *Forests*, vol. 6, pp. 3197–3211, 2015, doi: 10.3390/f6093197.

[20] G. Cheng, X. Xie, J. Han, L. Guo, and G.-S. Xia, "Remote sensing image scene classification meets deep learning: Challenges, methods, benchmarks, and opportunities," *IEEE J. Sel. Topics Appl. Earth Observ. Remote Sens.*, vol. 13, pp. 3735–3756, Jun. 2020, doi: 10.1109/JSTARS.2020.3005403.

[21] M. G. Rollins, "LANDFIRE: A nationally consistent vegetation, wildland fire, and fuel assessment," *Int. J. Wildland Fire*, vol. 18, pp. 235–249, 2009, doi: 10.1071/WF08088.

[22] T. Curt, "Fire frequency," in *Encyclopedia of Wildfires and Wildland-Urban Interface (WUI) Fires*. Cham, Switzerland: Springer, 2018, doi: 10.1007/978-3-319-51727-8_110-1.

[23] E. K. Brown, J. Wang, and Y. Feng, "US wildfire potential: A historical view and future projection using high-resolution climate data," *Environ. Res. Lett.*, vol. 16, no. 3, Mar. 2021, Art. no. 034060, doi: 10.1088/1748-9326/aba868.

[24] D. Phiri, M. Simwanda, S. Salekin, V. R. Nyirenda, Y. Murayama, and M. Ranagalage, "Sentinel-2 data for land cover/use mapping: A review," *Remote Sens.*, vol. 12, Jul. 2020, Art. no. 2291, doi: 10.3390/rs12142291.

[25] "Moisture deficit and surplus 2000–2022," ArcGIS, May 2024. [Online]. Available: https://www.arcgis.com/home/item.html?id=5cc1f9b53fa14f38b92b4bf76d49cca7

[26] C. H. Homer, J. A. Fry, and C. A. Barnes, "The national land cover database," U.S. Geological Surv. Fact Sheet 2012-3020, Feb. 2012.

[27] O. Ronneberger, P. Fischer, and T. Brox, "U-Net: Convolutional networks for biomedical image segmentation," in *Medical Image Computing and Computer-Assisted Intervention*. Cham, Switzerland: Springer, 2015, pp. 234–241.

[28] L. Chen, G. Papandreou, F. Schroff, and H. Adam, "Rethinking atrous convolution for semantic image segmentation," 2017.

[29] H. Zhao, J. Shi, X. Qi, X. Wang, and J. Jia, "Pyramid scene parsing network," in *Proc. IEEE Conf. Comput. Vis. Pattern Recognit.*, Honolulu, HI, USA, 2017, pp. 6230–6239, doi: 10.1109/CVPR.2017.660.

[30] A. Kirillov, Y. Wu, K. He, and R. Girshick, "PointRend: Image segmentation as rendering," in *Proc. IEEE/CVF Conf. Comput. Vis. Pattern Recognit.*, 2020, pp. 9796–9805, doi: 10.1109/CVPR42600.2020.00982.

[31] H. Wang, F. Yu, J. Xie, H. Wang, and H. Zheng, "Road extraction based on improved DeepLabV3 Plus in remote sensing image," *Int. Arch. Photogramm., Remote Sens. Spatial Inf. Sci.*, vol. 48, pp. 67–72, 2022, doi: 10.5194/isprs-archives-XLVIII-3-W2-2022-67-2022.

[32] A. Farasin, L. Colomba, and P. Garza, "Double-step U-Net: A deep learning-based approach for the estimation of wildfire damage severity through Sentinel-2 satellite data," *Appl. Sci.*, vol. 10, no. 12, Jun. 2020, Art. no. 4332, doi: 10.3390/app10124332.

[33] F.-J. Pérez-Porras, P. Trivino-Tarradas, C. Cima-Rodriguez, J.-E. Merono-de-Larriva, A. Garcia-Ferrer, and F.-J. Mesas-Carrascosa, "Machine learning methods and synthetic data generation to predict large wildfires," *Sensors*, vol. 21, no. 1, May 2021, Art. no. 3694, doi: 10.3390/s21113694.

[34] S. Kondylatos et al., "Wildfire danger prediction and understanding with deep learning," *Geophys. Res. Lett.*, vol. 49, Sep. 2022, Art. no. e2022GL099368, doi: 10.1029/2022GL099368.

[35] M. Seddouki, M. Benayad, Z. Aamir, M. Tahiri, M. Maanan, and H. Rhinane, "Using machine learning coupled with remote sensing for forest fire susceptibility mapping. Case study Tetouan Province, Northern Morocco," *Int. Arch. Photogramm. Remote Sens. Spatial Inf. Sci.*, vol. XLVIII-4/W6-2022, pp. 333–342, Nov. 2022.

[36] D. Wang, J. Zhang, B. Du, G.-S. Xia, and D. Tao, "An empirical study of remote sensing pretraining," *IEEE Trans. Geosci. Remote Sens.*, vol. 61, 2023, Art. no. 5608020, doi: 10.1109/TGRS.2022.3176603.

[37] M. P. Thompson and D. E. Calkin, "Uncertainty and risk in wildland fire management: A review," *J. Environ. Manage.*, vol. 92, no. 8, pp. 1895–1909, Aug. 2011, doi: 10.1016/j.jenvman.2011.03.015.

[38] M. J. Myer, K. A. Vanselow, and C. Samini, "Fire regimes at the arid fringe: A 16-year remote sensing perspective (2000–2016) on the controls of fire activity in Namibia from spatial predictive models," *Ecol. Indicators*, vol. 91, pp. 324–337, Aug. 2018, doi: 10.1016/j.ecolind.2018.04.022.

[39] L. Giglio, T. Loboda, D. P. Roy, B. Quayle, and C. O. Justice, "An active-fire based burned area mapping algorithm for the MODIS sensor," *Remote Sens. Environ.*, vol. 113, no. 2, pp. 408–420, Feb. 2009, doi: 10.1016/j.rse.2008.10.006.

[40] W. J. Bond and J. E. Keeley, "Fire as a global 'herbivore': The ecology and evolution of flammable ecosystems," *Trends Ecol. Evol.*, vol. 20, no. 7, pp. 387–394, Jul. 2005, doi: 10.1016/j.tree.2005.04.025.

[41] C. Meng, "Nutrient availability and microbial traits constrained by soil texture modulate the impact of forest fire on gross nitrogen mineralization," *Forestry Ecol. Manage.*, vol. 541, Aug. 2023, Art. no. 121067, doi: 10.1016/j.foreco.2023.121067.

Riya Gupta is currently a Senior with Northwood High School, Irvine, CA, USA. She carried out this research as a NASA SEES intern in partnership with the University of Toledo, GLOBE Mission Earth, and NASA Langley Research Center. She was mentored by Dr. Yitong Jiang and Dr. Kevin Czajkowski of the University of Toledo. She is interested in the applications of machine learning, material science, and e-textiles to space technology.

Hudson Kim is currently a Senior with Westview High School, San Diego, CA, USA. In 2023, he was a NASA SEES intern, developing geospatial machine learning models in collaboration with the University of Toledo, GLOBE Mission Earth, and NASA Langley Research Center. His research interests include humanoid robots, ion thrusters, satellite imagery, and remote sensing. He is a current intern with Kneron, San Diego, CA, USA, working on autonomous drone navigation and indoor mapping with VSLAM.